

Fabrication and characterization of nano-bridge Josephson junction based on $\text{Fe}_{0.94}\text{Te}_{0.45}\text{Se}_{0.55}$ thin film

Jia Lu¹, Wen Zhang², Zheng Wang², Xiaoming Ma^{1,3}, Shicai Shi², Lei Yan^{1*}, Hong Ding^{1,4}

¹Beijing National Laboratory for Condensed Matter Physics and Institute of Physics, Chinese Academy of Sciences, 3rd South Street, Zhongguancun, Beijing, 100190, China

²Purple Mountain Observatory and Key Laboratory of Radio Astronomy, Chinese Academy of Sciences, No.2 West Beijing Road, Nanjing, Jiangsu, 210008, People's Republic of China

³Department of Physics, Southern University of Science and Technology (SUSTech), No. 1088 Xueyuan Road, Shenzhen, Guangdong, 518055, China

⁴CAS Center for Excellence in Topological Quantum Computation, University of Chinese Academy of Sciences, 3rd South Street, Zhongguancun, Beijing, 100190, China

*Corresponding author: Tel: (+86) 10-82649538; E-mail: lyan@iphy.ac.cn

DOI: 10.5185/amlett.2019.2270

www.vbripress.com/aml

Abstract

Nano-bridge Josephson junction has been fabricated with $\text{Fe}_{0.94}\text{Te}_{0.45}\text{Se}_{0.55}$ (FTS) thin films by using focused ion beam etching (FIB). Electrical properties of the Josephson effects of the nano-bridge have been deeply studied. Current-voltage (I - V) characteristics of the junction exhibit resistively and capacitively shunted junction-like (RCSJ) behaviors. Critical current of the junction is 16.1 mA at 4.2 K. The product of the critical current and normal state resistance ($I_c R_n$) is higher than those reported in the literatures. Thermal conductance of the nano-bridge increases with increasing resistance, which suggests that the thermal transfer has been enhanced. Noise equivalent power of the nano-bridge is at the order of magnitude of 10^{-12} WHz^{-1/2}, which is comparable to that of the NbN bolometer. With these unique electrical characteristics, the FTS based nano-bridge could have various potential applications. Copyright © 2019 VBRI Press.

Keywords: Nano-bridge Josephson junction, iron-based superconductor.

Introduction

The Josephson effects (JEs) were first proposed by Brian D. Josephson in 1962, which were then confirmed by experiments. The JEs describe the transfer of Cooper pairs and the coupling of the macroscopic wave functions between two superconductors through a weak link. These effects are helpful to study the multiple energy gaps and the symmetry of superconducting order parameters [1-4], the nature of the Cooper pair coupling mechanism and the applications of superconducting electronics [5-7]. Several types of Josephson junctions have been proposed for fundamental experimental studies, such as point contacts, grain boundary junctions and hybrid junctions with a structure of superconductor-normal metal-superconductor (SNS). The iron based superconductors have attracted great interests since their discovery [8-10]. Josephson junctions based on iron based superconductors have been widely and extensively studied. Zhang *et al.* reported the first Josephson effects based on doped BaFe_2As_2 (Ba-122) single crystal, with Pb counter electrode along the c-axis in both planar and

point-contact geometries [11]. In that study, conventional Josephson behavior was observed, with the presence of resistively and capacitively shunted junction (RCSJ) type current-voltage (I - V) behavior and sharp Shapiro steps. They also studied the JEs between electron-doped and hole-doped iron pnictide single crystals [12]. The intergrain critical current density across the grain boundaries in iron pnictide superconductors has been extensively explored [13-16]. The first thin film Josephson junction with Ba-122 was realized on the (La,Sr)(Al,Ta)O₃ bicrystals by Katase *et al.* [13, 14] RCSJ like I - V characteristics were observed up to 17 K, while the $I_c R_n$ product was only 60 mV at 4.2 K. Schmidt *et al.* reported hybrid planar thin film based SNS Josephson junctions in c-axis direction [17-19]. It has been concluded that planar junctions have various advantages than other junction structures, such as capability of controlling electrical properties and simple fabrication process. However, bridge type junctions have been rarely reported. Wu's group was among the first to study the transport properties and dc/ac JEs of FeTeSe nano-bridge [20]. They fabricated nano-bridges from

248 to 672 nm by using the FIB process. The critical currents of these nano-bridges increased as the width of the bridge was increased. Also, the I - V characteristics can be fitted by using the RSCJ-model. They examined the effect of microwave irradiation on properties of the junctions. It was found that the sharpness of the superconducting phase transition could be utilized for radiation detection [21, 22]. For instance, a thermometer was fabricated with an SNS Josephson junction, which had high sensitivities [23].

In this regard, it is expected that FTS planar Josephson junctions should be potential candidates for such applications. In this letter, nano-bridge junction based on FTS thin films was developed by using FIB method, which displayed weak coupling effect. In addition, thermal characteristics of the junction has been evaluated.

Experimental

The FTS thin films on (100) SrTiO₃ substrates were deposited by using pulsed laser deposition (PLD) from a bulk FTS target, which was offered by Gu's group [24, 25]. The FTS films have been deposited at high vacuum levels, at a pressure of 5×10^{-6} Pa and a substrate temperature of 450 °C. The thickness of thin film is approximate 120 nm, which was confirmed by using scanning electron microscope (SEM) (FEI XL30S). Crystal structures and orientations of the FTS thin film were characterized by using X-ray diffraction (XRD) in θ - 2θ scan mode, with Cu K _{α} radiation (Model: Bruker D8 system).

The FTS nano-bridge was then directly prepared by using the focused ion beam (FIB) (Model: FEI DB235) process [28, 29]. Firstly, Pt layer with a dimension of $2 \mu\text{m} \times 2 \mu\text{m}$ was coated on the FTS thin film by using FIB to protect its surface and reduce the damage caused by containment of the gallium ions. To form junctions, FTS nano-bridge with width less than $1 \mu\text{m}$ was subsequently formed through FIB etching.

Resistivity of the nano-bridge was measured by using a physical property measurement system (PPMS) (Model: Quantum Design Model 6000) at temperatures ranging from room temperature to 2K. I - V characteristics and thermal conductance of the device were measured by using an Oxford Triton 400 dilution cooler.

Results and discussion

Fig. 1 shows XRD pattern of the FTS thin film. Since only (00 l) peaks can be distinguished, the FTS film is well epitaxially grown with (001) orientation onto the STO substrate. In order to estimate the superconductivity, the dependence of electrical resistance on temperature (R - T) of the thin film has been measured, as shown in **Fig. 2**. The critical temperature (T_c) is 14.3 K, close to the T_c value of FTS bulk and films reported earlier [26, 27]. In other words, our FTS thin film has typical superconductor properties.

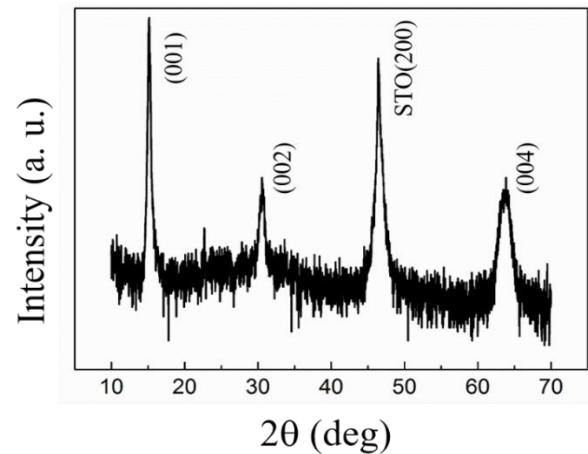


Fig. 1. XRD pattern of the FTS thin film deposited on SrTiO₃ (100).

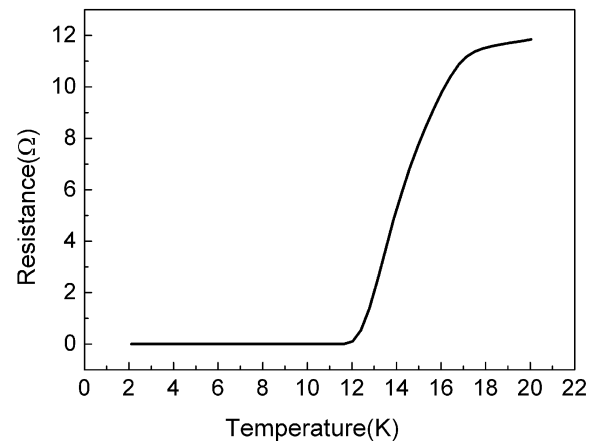


Fig. 2. Temperature dependence of electrical resistance of the FTS thin film.

Fig. 3 presents SEM image of the nano-bridge structure with a width of 860 nm. The entire film is divided into two parts, only connected by a bridge structure marked with the dot line.

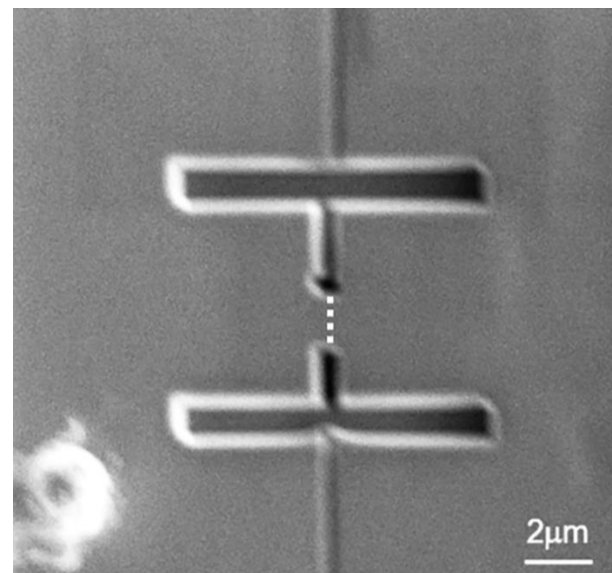


Fig. 3. SEM image of the FTS nano-bridge fabricated by using FIB.

Fig. 4a shows I - V characteristic of the FTS nano-bridge measured at 4.2 K. The electrical properties are similar to the results reported in [20]. This FTS based JEs junction is in a good agreement with the typical RCSJ model, which means that the intergrain coupling of the FTS nano-bridge belongs to Josephson type. The critical current of the junction, I_c , is about 16.1 mA, with a pronounced asymmetry. Similar results were reported in [20], where the critical current increases with increasing width of the nano-bridge. This asymmetry could be attributed to the flux trapped in the junction. Extrapolating the linear part of the I - V curves in **Fig. 4a** to zero voltage gives rise to an excess current, I_{ex} , with a value of about 13.5 mA, which is lower than I_c . The normal resistance (R_n) of the nano-bridge directly obtained from the I - V curve is about 11.2 Ohm, nearly twice that reported in [20]. The $I_c R_n$ product of the junction is about 180 mV. The values is much larger than that reported in the literature [15, 16, 20], which indicates that our nano-bridge with large R_n and $I_c R_n$ is suitable for high frequency applications, as compared with the other junction structures [30].

The relationship between critical current (I_c) and the temperature from 2.5 K to 15 K is shown in **Fig. 4b**. The critical current changes from 16.1 mA to 14.3 mA, as the temperature is raised from 2.5 to 7 K. The I_c value of the nano-bridge changes only very slightly as the temperature is below 7 K, which is half of the critical temperature. This nano-bridge exhibits stable superconducting properties below the half of T_c .

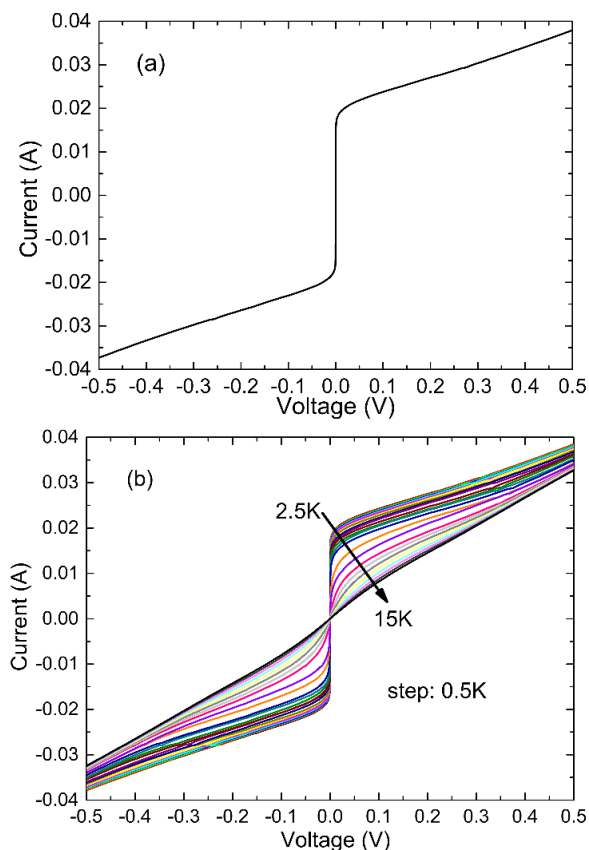


Fig. 4. (a) I - V curve of the FTS nano-bridge at $T=4.2$ K (b) I - V curves of FTS nano-bridge at different temperatures.

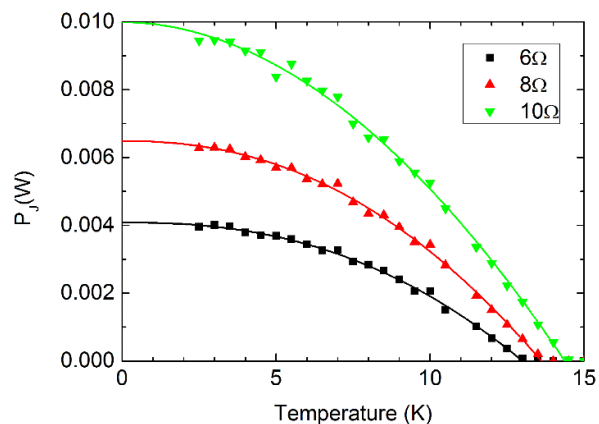


Fig. 5. Power level of the FTS nano-bridge as a function of bath temperature.

The FTS thin film has higher critical temperature than Nb, thus reducing the cooling power, which is very important for some special applications. Meanwhile, the FTS nano-bridge has large R_n and $I_c R_n$, making it possible for the application as bolometers. When the bolometer is used in constant current mode, the electrical resistance change modifies the DC joule power, producing an effective thermal conductance. The I - V characteristics of the nano-bridge at different bath temperatures from 2.5 K to 15 K were measured. The data points of the I - V curves at 6, 8 and 10 Ω were selected. The power level as a function of bath temperature is plot in **Fig. 5** [31, 32]. The obtained T_c is consistent with the value previously measured from the R - T curve. The data points are fitted to the heat balance equation [33]:

$$P_{joule} = K(T_c^n - T^n), \tag{1}$$

where, K is a constant that depends on geometry and material properties of the FTS nano-bridge, while n is the thermal conductance exponent, which depends on the dominant thermal transport mechanism. For this device, a best fit can be obtained for the selected resistance values (see **Table 1**). The thermal transport parameters are $n=2.4$, $K=0.875$ WK^{-n} and $T_c = 13K$ at 6 Ω . The obtained parameters increase with increasing resistance value from 6 to 10 Ω , which indicates that the thermal transfer process is not only affected by the nano-bridge itself but also is related to the contact electrode at low temperatures.

Table 1. Thermal transfer parameters for different resistance values of the FTS nano-bridge.

Resistance	6 Ω	8 Ω	10 Ω
Parameters			
$K(10^{-5} WK^{-n})$	0.875	1.912	5.485
T_c (K)	13	13.61	14.369
n	2.396	2.232	1.953
$G(10^{-3} WK^{-1})$	0.753	1.063	1.356
$NEP(10^{-12} WHZ^{-1/2})$	1.874	2.33	2.78

The thermal conductance between FTS nano-bridge and STO substrate is therefore obtained with $G = nKT_c^{n-1}$ [31]. G also increases with increasing resistance value over the range of 6-10 Ω , indicating an enhancement of thermal transport. This can be attributed to the fact that the hot electron temperature of the nano-bridge with higher resistance is raised due to the dc power and that heat is transferred to substrate through electron-phonon interaction and electron diffusion, while only electron-phonon interaction plays a dominant role in the case of lower resistance.

For a bolometer, the noise consists of thermal fluctuation noise, Johnson noise and related amplifier noise [34, 35]. The sensitivity of a bolometer is determined by its thermal fluctuation noise. Noise equivalent power (NEP) [31] can be expressed as $NEP = \sqrt{4k_B T_c^2 G}$. The calculated NEP shows a value at the scale of 10^{-12} $WHz^{-1/2}$, which is comparable with that of the NbN bolometer [35], confirming that our FTS nano-bridge has potential applications as such highly sensitive detector devices. The increase in NEP with increasing resistance is mostly attributed to the reduction in sensitivity due to the higher thermal conductance.

Conclusions

In summary, FTS nano-bridge junction with a width of 860 nm on STO substrate has been made by using FIB technique. It is found that the critical current of the nano-bridge increases with decreasing temperature, with a critical current of 16.1 mA at 4.2 K. DC joule power of the nano-bridge, with a constant resistance at different temperatures, could be fitted by using the heat balance equation. The hot electron temperature of the nano-bridge with higher resistance is raised due to the DC power. The thermal conductance (G) is about $1 \times 10^{-3} W \cdot K^{-1}$. The noise equivalent power value of the nano-bridge is comparable with that of the NbN bolometer, which should be further improved for real applications. The performance of this FTS nano-bridge at high frequencies will be thoroughly studied in our future work.

Acknowledgements

This work was supported by Chinese Academy of Sciences (Project No. XDB07030300) and National Key R&D Plan (Grants No. 2016YFA0401000). The authors thank Professor Genda Gu of Brookhaven National Laboratory for providing high-quality FTS targets.

Author's contributions

Lei Yan and Hong Ding designed the project. Jia Lu prepared the FTS thin film and the nano-bridge structure under the guidance of Lei Yan and Hong Ding. Shengcai Shi, Wen Zhang and Zheng Wang were responsible for the measurement of resistivity and thermal transport of the samples. Jia Lu, Wen Zhang and Xiaoming Ma analyzed the data. Jia Lu and Wen Zhang prepared the manuscript. The authors have no competing financial interests.

References

- Yin, Y.; Zech, M.; Williams, T.L.; Wang, X.F.; Wu, G.; Chen, X. H.; Hoffman, J. E., *Phys. Rev. Lett.*, **2009**, *102*, 097002.
DOI: 10.1103/PhysRevLett.102.097002
- Massee, F.; Huang, Y.; Huisman, R.; Jong, S.; Goedkoop, J. B.; Golden, M. S., *Phys. Rev. B*, **2009**, *79*, 220517(R).
DOI: 10.1103/PhysRevB.79.220517
- Zhang, X.; Oh, Y. S.; Liu, Y.; Yan, L.; Saha, S. R.; Butch, N. P.; Kirshenbaum, K.; Kim, K. H.; Paglione, J.; Greene, R. L.; Takeuchi, I., *Phys. Rev. B*, **2010**, *82*, 020515(R).
DOI: 10.1103/PhysRevLett.102.147002
- Ota, Y.; Machida, M.; Koyama, T.; Matsumoto, H., *Phys. Rev. Lett.*, **2009**, *102*, 237003.
DOI: 10.1103/PhysRevLett.102.237003
- Buckel, W.; Kleiner, R., *Superconductivity 2nd Edition*; Wiley: Weinheim, **2004**.
DOI: 10.1002/9783527618507
- Gallop, J.C., *SQUIDS, the Josephson Effects and Superconducting Electronics*; Bristol: Hilger, **1992**.
DOI: 10.1002/19920040720
- Clarke, J.; Braginski, A., *The SQUID Handbook Vol. 2*; Wiley: Weinheim, **2006**.
DOI: 10.1002/9783527609956
- Kamihara, Y.; Watanabe, T.; Hirano, M.; Hosono, H., *J. Am. Chem. Soc.*, **2008**, *130*, 3296.
DOI: 10.1021/ja800073m
- Chen, G. F.; Li, Z.; Li, G.; Zhou, J.; Wu, D.; Dong, J.; Hu, W.Z.; Zheng, P.; Chen, Z. J.; Yuan, H. Q.; Singleton, J.; Lou, J. L.; Wang, N. L., *Phys. Rev. Lett.*, **2008**, *101*, 057007.
DOI: 10.1103/PhysRevLett.101.057007
- Ren, Z. A.; Lu, W.; Yang, J.; Yi, W.; Shen, X.; Li, Z. C.; Che, G. C.; Dong, X.L.; Sun, L.L.; Zhou F.; Zhao, Z. X., *Chin. Phys. Lett.*, **2008**, *25*, 2215.
DOI: 10.1088/0256-307X/25/6/080
- Zhang, X.; Oh, Y. S.; Liu, Y.; Yan, L. Q.; Kim, K. H.; Greene, R. L.; Takeuchi, I., *Phys. Rev. Lett.*, **2009**, *102*, 147002.
DOI: 10.1103/PhysRevLett.102.147002
- Zhang, X.; Saha, S. R.; Butch, N. P.; Kirshenbaum, K.; Paglione, J.; Greene, R. L.; Liu, Y.; Yan, L.; Oh, Y. S.; Kim, K. H.; Takeuchi, I., *Appl. Phys. Lett.*, **2009**, *95*, 062510.
DOI: 10.1063/1.3205123
- Katase, T.; Ishimaru, Y.; Tsukamoto, A.; Hiramatsu, H.; Kamiya, T.; Tanabe, K.; Hosono, H., *Appl. Phys. Lett.*, **2010**, *96*, 142507.
DOI: 10.1063/1.3371814
- Katase, T.; Ishimaru, Y.; Tsukamoto, A.; Hiramatsu, H.; Kamiya, T.; Tanabe, K.; Hosono, H., *Supercond. Sci. Technol.*, **2010**, *23*, 082001.
DOI: 10.1088/0953-2048/23/8/082001
- Lee, S.; Jiang, J.; Weiss, J. D.; Folkman, C. M.; Bark, C. W.; Tarantini, C.; Xu, A.; Abraimov, D.; Polyanskii, A.; Nelson, C. T.; Zhang, Y.; Baek, S. H.; Jang, H. W.; Yamamoto, A.; Kametani, F.; Pan, X. Q.; Hellstrom, E. E.; Gurevich, A.; Eom, C. B.; Larbalestier, D. C., *Appl. Phys. Lett.*, **2009**, *95*, 212505.
DOI: 10.1063/1.3262953
- Lee, S.; Jiang, J.; Zhang, Y.; Bark, C. W.; Weiss, J. D.; Tarantini, C.; Nelson, C. T.; Jang, H. W.; Folkman, C. M.; Baek, S. H.; Polyanskii, A.; Abraimov, D.; Yamamoto, A.; Park, J. W.; Pan, X. Q.; Hellstrom, E. E.; Larbalestier, D. C.; Eom, C. B., *Nat. Mater.*, **2010**, *9*, 397.
DOI: 10.1038/NMAT2721
- Schmidt, S.; D'oring, S.; Schmidl, F.; Grosse, V.; Seidel, P.; Iida, K.; Kurth, F.; Haindl, S.; M'onch, I.; Holzappel, B., *Appl. Phys. Lett.*, **2010**, *97*, 172504.
DOI: 10.1063/1.3505526
- D'oring, S.; Schmidt, S.; Schmidl, F.; Tympel, V.; Haindl, S.; Kurth, F.; Iida, K.; M'onch, I.; Holzappel, B.; Seidel, P., *Physica C*, **2012**, *478*, 15.
DOI: 10.1016/j.physc.2012.03.030
- Reifert, D.; Hasan, N.; D'oring, S.; Schmidt, S.; Monecke, M.; Feltz, M.; Schmidl, F.; Tympel, V.; Wisniewski, W.; M'onch, I.; Wolf, T.; Seidel, P., *Supercond. Sci. Technol.*, **2014**, *27*, 085003.
DOI: 10.1088/0953-2048/27/8/085003.

20. Wu, C. H.; Chang, W. C.; Jeng, J. T.; Wang, M. J.; Li, Y. S.; Chang, H. H.; Wu, M. K.; *Appl. Phys. Lett.*, **2013**, *102*, 222602.
DOI: 10.1063/1.4809920
21. Golubev, D. S.; Kuzmin, L. S., *J. Appl. Phys.*, **2001**, *89*, 6464.
DOI: 10.1063/1.1351002
22. Kuzmin, L., *Microelectron. Eng.*, **2003**, *69*, 309.
DOI: 10.1016/S0167-9317(03)00314-9
23. Govenius, J.; Lake, R. E.; Tan, K. Y.; Pietila, V.; Julin, J. K.; Maasilta, I. J.; Virtanen, P.; Mottonen, M., *Phys. Rev. B*, **2014**, *90*, 064505.
DOI: 10.1103/PhysRevB.90.064505
24. Bellingeri, E.; Buzio, R.; Gerbi, A.; Marre^{*}, D.; Congiu, S.; Cimberle, M. R.; Tropeano, M.; Siri, A. S.; Palenzona, A.; Ferdeghini, C., *Supercond. Sci. Technol.*, **2009**, *22*, 105007.
DOI:10.1088/0953-2048/22/10/105007
25. Bellingeri, E.; Pallecchi, I.; Buzio, R.; Gerbi, A.; Marre, D.; Cimberle, M. R.; Tropeano, M.; Putti, M.; Palenzona, A.; Ferdeghini, C., *Appl. Phys. Lett.*, **2010**, *96*, 102512.
DOI: 10.1063/1.3358148
26. Sales, B. C.; Sefat, A. S.; McGuire, M. A.; Jin, R. Y.; Mandrus, D.; Mozharivskiy, Y., *Phys. Rev. B*, **2009**, *79*, 094521.
DOI: 10.1103/PhysRevB.79.224524
27. Si, W.; Lin, Z. W.; Jie, Q.; Yin, W.-G.; Zhou, J.; Gu, G.; Johnson, P. D.; Li, Q., *Appl. Phys. Lett.*, **2009**, *95*, 052504.
DOI: 10.1063/1.3195076
28. Neumann, C.; Yamaguchi, K.; Hayashi, K.; Suzuki, K.; Enomoto, Y.; Tanaka, S., *Physica C*, **1993**, *210*, 138.
DOI: 10.1016/0921-4534(93)90018-L
29. Chen, C.-H.; Trajanovic, Z.; Dong, Z. W.; Lobb, C. J.; Venkatesan, T.; Edinger, K.; Orloff, J.; Melngailis, J.; *J. Vac. Sci. Technol. B*, **1997**, *15*, 2379.
DOI:10.1116/1.589651
30. Sarnelli, E.; Adamo, M.; Nappi, C.; Braccini, V.; Kawale, S.; Bellingeri, E.; Ferdeghini, C.; *Appl. Phys. Lett.*, **2014**, *104*, 162601.
DOI: 10.1063/1.4871864
31. Wei, J.; Olaya, D.; Karasik, B.S.; Pereverzev, S.V.; Sergeev, A.V.; Gershenson, M. E.; *Nat. Nanotechnol.*, **2008**, *3*, 496.
DOI:10.1038/nnano.2008.173
32. Zhang, W.; Zhong, J. Q.; Miao, W.; Wang, Z.; Liu, D.; Yao, Q. J.; Shi, S. C.; Chen, T. J.; Wang, M. J., *J. Low. Temp. Phys*, **2016**, *184*, 11.
DOI: 10.1007/s10909-015-1352-4
33. Kooi, J. W.; Baselmans, J. J. A.; Hajenius, M.; Gao, J. R.; Klapwijk, T. M.; Dieleman, P.; Baryshev, A.; Lange, G., *J. Appl. Phys.*, **2007**, *101*, 044511.
DOI: 10.1063/1.2400086
34. Miao, W.; Zhang, W.; Zhou, K. M.; Zhang, K.; Duan, W. Y.; Yao, Q. J.; Shi, S. C., *IEEE. Trans. Appl. Supercond.*, **2013**, *23*, 2300104.
DOI: 10.1109/TASC.2012.2229777
35. Liu, D.; Li, J.; Wang, Z.; Yao, M.; Hu, J.; Shi, S. C., *IEEE. Trans. Appl. Supercond.*, **2013**, *23*, 1400504.
DOI: 10.1109/TASC.2012.2237493
36. Zhang, W., Miao, W.; Zhou, K. M.; Li, S. L.; Lin, Z. H.; Yao, Q. J.; Shi, S.C., *IEEE. Trans. Appl. Supercond.*, **2011**, *21*, 3.
DOI:10.1109/TASC.2010.20975